Study on elastic deformation calculation method of a composite-metal hybrid assembling stringed truss bridge

Zeng Zigang[1], Chen Li[2],*, Zhao Dong[1], Mao Haifeng[3], Zhang Dongdong[4], Zhao Qilin[3]

[1]Research Institute of Engineering Design, Armed Police Force Research Academy, 100000 Beijing, China

[2]School of Economics &Management, Nanjing Institute of Technology, 211167 Nanjing, China

[3]School of Mechanical and Power Engineering, Nanjing Tech University, 211816 Nanjing, China

[4] College of Field Engineering, Army Engineering University of PLA, 210007 Nanjing, China

Abstract. A composite-metal hybrid assembling stringed truss bridge which based on pre-tightened tooth connection can make full use of the strength of the FRP fiber in the direction of the fiber, and is of higher bearing capacity than the FRP truss bridges with traditional adhesive or bolt connection. However, whether the calculation method of FRP truss bridge with traditional bonding or bolt connection is suitable for this new type of bridge needs to be researched because of the difference on the structural form and connection mode. In order to obtain the suitable method of this kind of bridge, a new method for calculating live load deformation which consider the influence of end of the steel bar sleeve of rod stiffness was established in this paper; the deformation experiment of truss bridge was carried out. The experiment and calculation results show: compared with the calculation method of the live load deformation of the traditional FRP truss bridge, the calculation method of live load deformation considering the effect of the steel sleeve on the end of the rod is in good agreement with the live load deformation obtained by the experiment; the calculation method of inelastic deflection has also been verified by the experimental results.

1 Introduction

FRP truss bridge which can make full advantage of high specific strength and stiffness along fiber direction of FRP materials has been widely recognized by researchers at home and abroad. There are many successful engineering cases, such as Swiss Pontresina bridge[1], Danish Kolding bridge[2], Japanese Iwao Sasaki bridge[3] and Greek Kostopoulos bridge[4,5]. using FRP section extrusion on structural members which connected by traditional glue, bolt or metal plate with bolts. The traditional design and calculation method of steel and concrete structure[6,7] is often used in FRP truss bridge, and the finite-element(FE) software is used for modeling and calculation. Due to the complexity of the actual structure, it is necessary to use simplified FE model instead of solid FE model in the calculation of deformation. A link element or beam element with a single material is simulated as the member bar, and the joints are assumed as hinged or rigid[8]. The calculation accuracy of this deformation calculation method can generally meet the requirements.

Zhao Qilin et al.[10,11] have developed a kind of assembling stringed truss bridge based on FRP and metal material combination of pre-tightened teeth joint. Unlike the usual FRP truss bridge, a longer steel sleeve is wrapped around the end of the FRP member of the truss bridge, and the steel sleeve and the metal plate are welded to form a joint. Compared with the bonded or bolted FRP truss bridges mentioned above, the composite-metal hybrid assembling stringed truss bridge can give better play to the along-fiber strength of FRP materials, so they have higher bearing capacity[12,13]. The tensile and compressive stresses of the bonded or bolted FRP truss members are generally only tens of MPa, while the tension and compression stresses of the composite-metal hybrid assembling stringed truss bridge can exceed 300MPa. However, due to the existence of steel sleeve at the end of FRP member, the stiffness at the end of FRP member of the truss bridge is obviously enhanced. Therefore, it's necessary to study whether the deformation calculation method used in the above-mentioned bonded or bolted FRP truss bridge is suitable for the composite-metal hybrid assembling stringed truss bridge.

In this paper, the deformation calculation method of the composite-metal hybrid assembling stringed truss bridge is studied. Based on the analysis of the structural differences between composite-metal hybrid assembling stringed truss bridge and traditional FRP bridge, a new method is proposed by considering the influence of the steel sleeve at the end of the member on the stiffness of the member. Finally, the results of the above method are compared with those of the traditional method and experiment.

2 Structure of the bridge

2.1 Main structure

The truss bridge structure is composed of FRP-metal hybrid space truss with a length of 54m and a width of 3.2m as shown in Fig. 1. It is composed of 7 standard sections and 2 side sections with a length of 6m. The main standard bridge section truss is 1.2m high. The main girder has a string which is 2.0m high. The total weight of the truss bridge is 13.5 tons. The design load of the bridge is 20 tons in total weight and 15 tons in single axle load. The upper chord and bridge deck are made of aluminum alloy, which is easy to bear the direct friction and impact of wheel or track, while the lower chord, vertical bar, oblique-vertical bar and oblique-web bar, which are mainly

* Corresponding author: Chen Li, E-mail: alexandermacedonia@163.com.

Supports from the Science Foundation of Nanjing Institute of Technology (CKJB201506, YKJ201616) and the National Natural Science Foundation of China (51708552) are gratefully acknowledged.

subjected to unidirectional tension and compression load, are made up of FRP bars.

a) The composite-metal hybrid assembling stringed truss bridge

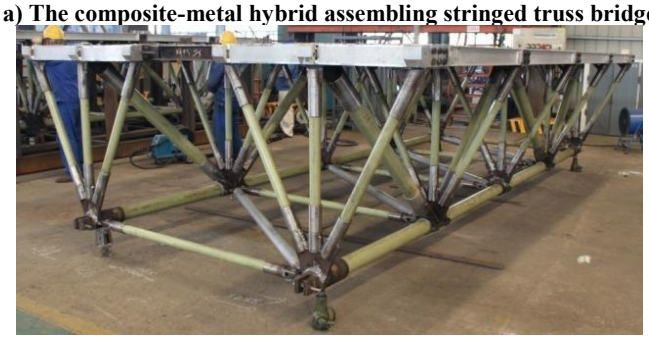

b) Standard bridge section

c) Side bridge section

Fig.1 Structure the composite-metal hybrid assembling stringed truss bridge

2.2 Joint

Composite-metal hybrid assembling stringed truss bridge differs from traditional FRP truss bridge in that its members are made up of composite materials, the joint of rods is made of pre-tightened teeth[14, 15], and the joint of truss segments is made of single-eared and double-eared joints.

The joint arrangement of the standard bridge section is shown in Figure 2. The pre-tightening teeth connecting joint at the end of the rod (Fig. 3) is a strip, ring and spiral tooth machined on the outer surface of the FRP pipe end, and matching teeth are machined on the metal parts connecting the composite components; then the metal parts are assembled with the composite components, and finally the radial pressure is applied on the composite teeth to form the joint with high load capacity. Since the pre-tightening teeth joint has a steel sleeve on the outer surface of the FRP pipe, it is convenient to weld the joint plate on the steel sleeve. The joints can be spliced together into a complete bridge section by welding different rods together. In the end of the rod, there is a section of the steel sleeve whose actual stiffness contribution should be considered. Two kinds of FRP tubes (G60, G104) are used in the structure. The size parameters and elastic modulus of the FRP tube and the corresponding steel sleeve are shown in Table 1. The elastic modulus of FRP bars is 52GPa, and that of steel sleeves is 206GPa. The stiffness of the composite section formed by the combination of them is much greater than that of FRP bars, that is, the stiffness of the end of the bar is greater than that of the middle. This is different from the general bonded or bolted truss. A much greater error may be caused in the FE results if the general truss FE method is used to calculate the deflection.

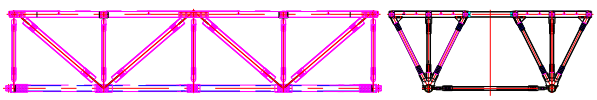

Fig.2 Joint layout of standard bridge section

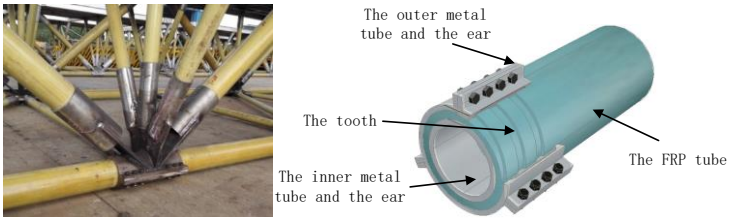

Fig.3 Pretensioning tooth joint for the composite-metal hybrid assembling stringed truss bridge

Tab 1 Basic parameters of GFRP tube and steel sleeve

	Outer diameter（mm）	Inner diameter（mm）	Elastic modulus（GPa）
G60 tube	60	48	52
G104 tube	104	88	52
G60 steel sleeve	72	60	206
G104 steel sleeve	128	104	206

3 Calculation method

3.1 Method of considering the stiffness of the end sleeve

The elastic deflection is calculated by ANSYS FE software. For the sake of simplicity, the beam and shell elements are used to establish the model. Beam188 is a 3-D 2-node element, which is suitable for analyzing slender to medium-thick beam structures. The deck is constructed with shell63 element which has both flexural and membrane forces, and can bear in-plane load and normal load, and each node of the shell element has six degrees of freedom. The transverse connection system is established by link180 element which has the axial tension and compression capacity. Each node the link element has three degrees of freedom. All degrees of freedom of the joint between the bridge section modules are coupled except the vertical degree of freedom. The model boundary at the both ends of side bridge section is simulated as simply supported degree of freedom.

The composite section at the end of the rod is converted into a single material section, and the section attributes are calculated according to the composite section. The end cross-section of the Pre-tightening teeth joint is shown in Figure 4. Considering the effect of the steel sleeve at the end of the bar on the stiffness, the section property of the steel sleeve at the end of the bar is modified to increase the stiffness in the finite element model. The material of the composite section to be modified is uniformly replaced by steel. Because the members of truss bridges are mainly subjected to tension and compression, the section area of the joints is determined by the principle of equivalent tension or compression stiffness (see Table 2 for basic parameters). The equivalent outer diameter of the section is consistent with the outer diameter of the original steel sleeve, and the inner diameter is determined by the equivalent area.

Equivalent area formula

$$A = \frac{E_1 A_1 + E_1 A_2 + E_2 A_3}{E_1} \tag{1}$$

Where:

E_1 --Elastic modulus of steel

A_1-- Section area of outer metal tube

A_2 -- Section area of inner metal tube

E_2-- Stiffness of FRP material

A_3 -- Sectional area of FRP tube

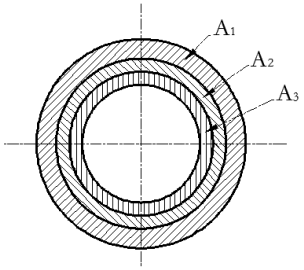

Fig. 4 Schematic diagram of connection section of truss bridge

In ANSYS model, the section attributes of the corresponding composite section at the end of the FRP member are modified to the section attributes of the converted section (Fig. 5). The elastic deflection considering the effect of the steel sleeve at the end of the member on the stiffness can be obtained by loading calculation.

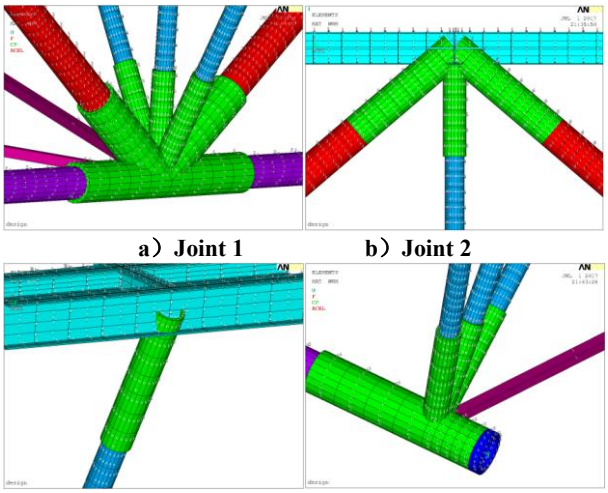

a）Joint 1 b）Joint 2

c）Joint 3 d）Joint 4

Fig.5 Connection diagram of truss bridge after equivalent replacement

As shown in Figure 6, five points at different positions located in 1/4 span of the bridge (D1 and D5), 1/3 span of the bridge(D2 and D4) and mid span of the bridge(D3). The calculated results of elastic deflection are shown in Table 3.1.

Table 2 Computational live load elastic deflection of truss bridge considering the effect of steel sleeve at the end of member on stiffness (mm)

Location	D1	D2	D3	D4	D5
2t	19.21	25.24	32.93	24.99	19.00
5t	48.02	63.10	82.33	62.48	47.50
7t	67.22	88.35	115.26	87.47	66.50
10t	96.04	126.21	164.65	124.96	94.99
12t	115.24	151.45	197.58	149.95	113.99
15t	144.06	189.31	246.98	187.44	142.49
17t	163.26	214.55	279.91	212.43	161.48
18t	172.87	227.17	296.38	224.93	170.98
20t	192.08	252.42	329.31	249.92	189.98
21t	201.68	265.04	345.77	262.41	199.48
23t	220.89	290.28	378.70	287.40	218.48

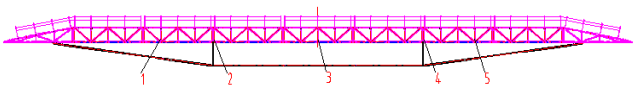

Fig. 6 Layout of displacement measuring points

4 Comparative analysis of theory and test

4.1 Test

In order to test the deformability of the bridge and verify the calculation method of elastic deflection and inelastic deflection, we carried out the loading test of the bridge. The test condition of the bridge is mid-span normal load, which is divided into six grades by staged loading. They are 2t, 7t, 12t, 17t, 20t and 23t respectively. The field loading test is shown in Figure 7.

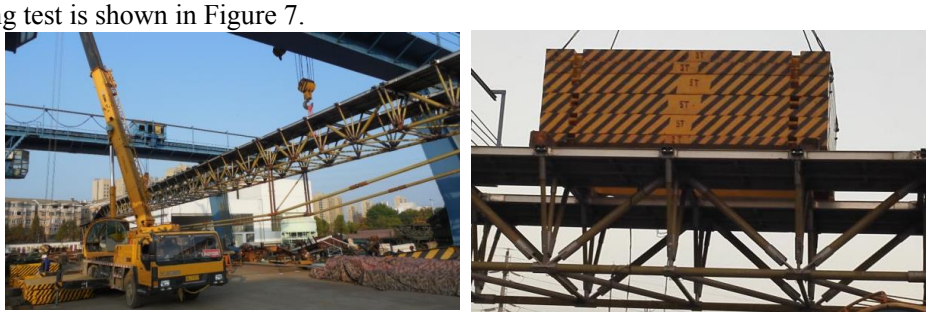

Fig. 7 Loading test photo under intermediate load condition

The upper truss of truss bridge should be kept horizontal before tensile test. The Total Station is used to measure the vertical displacement of the bridge, that is the live load deflection (the sum of the elastic deflection and the inelastic deflection). A total of 5 displacement measuring points are arranged on the bridge, with the same location as Figure 6. Measured deflection of the live load is shown in Table 3.

Table 3 Measured live load deflection of truss bridge (mm)

Location	2t	7t	12t	17t	20t	23t

D1	17.18	65.89	116.7	167.88	203.49	236.74
D2	27.2	93.43	162.87	232.94	280.83	325.52
D3	35.8	126.83	215.4	308.64	372.47	433.75
D4	24.2	91.06	155.95	223.71	271.36	316.36
D5	19.38	66.95	114.27	164.69	199.71	233.51

4.2 Elastic deflection comparison of theory and test by live loads

Since the measured live-load elastic deflection of truss bridges includes inelastic deflection and the magnitude of non-elastic deflection remains unchanged during loading, In order to get the measured live load elastic deflection of 5t, 10t, 15t, 18t and 21t, we can subtract the measured live-load deflection (elastic deflection + inelastic deflection) of 2t from the measured live-load deflection (elastic deflection + inelastic deflection) of 7t, 12t, 17t, 20t and 23t. The result is shown in Table 4.

The detailed comparison between live load test elastic deflection and measured deflection is shown in Figures 8 and 5. At the same time, in order to illustrate the difference between the calculation method of elastic deflection proposed in this paper and the calculation method of general FRP bridge elastic deflection (i.e. the finite element method without considering the influence of end steel sleeve on rigidity), the results of general FRP bridge live load elastic deflection are listed in Table 4.3, and compared with the two results mentioned above.

From the figure 8, it can be seen that the growth trend of the deflection calculated by this method is consistent with the measured deflection, and the results are in good agreement with each other.

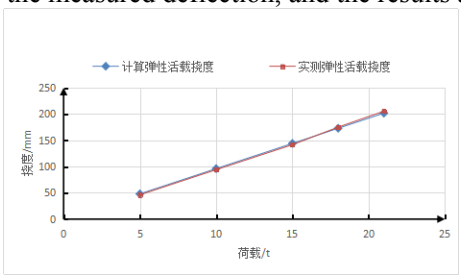

a) Live load elastic deflection of D1

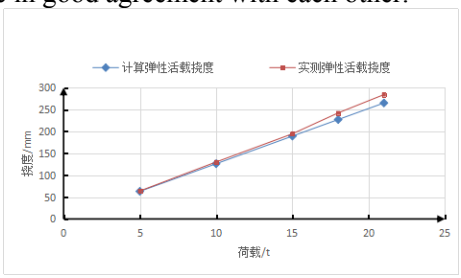

b) Live load elastic deflection of D2

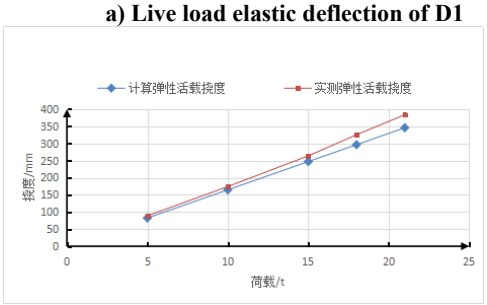

c) Live load elastic deflection of D3

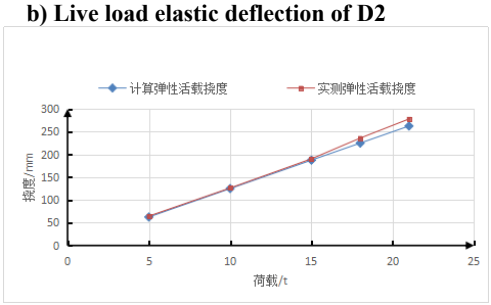

d) Live load elastic deflection of D4

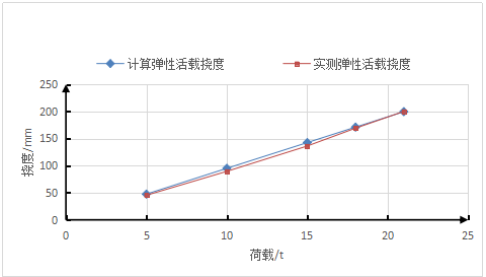

e) Live load elastic deflection of D5

Fig. 8 Live load elastic deflection diagram at each measuring point of truss bridge

From table 5, it can be seen that the average error rate of live load elastic deflection at 1/4 span (D1 and D5) is 18.61%(the maximum is 23.17%, the minimum is 13.67%) which can not be ignored, without considering the influence of steel sleeve at the end of the member on the stiffness. When considering the influence of steel sleeve at the end of the member on the stiffness, the average error rate of elastic deflection at the same place is 3.01%(the maximum is 7.40%, the minimum is 0.06%) which has been greatly reduced. The average error rate of live load elastic deflection at 1/3 span (D2 and D4) is 17.11%(the maximum is 22.94%, the minimum is 12.35%) without considering the influence of steel sleeve at the end of the member on the stiffness. When considering the influence of steel sleeve at the end of the member on the stiffness, the average error rate of elastic deflection at the same place is 1.55%(the maximum is 1.66%, the minimum is 0.21%). The average error rate of live load elastic deflection at 1/2 span (D3) is 18.66%(the maximum is 21.53%, the minimum is 15.18%) without considering the influence of steel sleeve at the end of the member on the stiffness. When considering the influence of steel sleeve

at the end of the member on the stiffness, the average error rate of elastic deflection at the same place is 5.07%(the maximum is 7.86%, the minimum is 2.78%). Considering the influence of steel sleeve at the end of the member on the stiffness, the error rate of live load elastic deflection of the truss bridge is within 10%, so the calculation method considering the influence of steel sleeve at the end of the member on the stiffness can be used to calculate the elastic deflection of the bridge under live load.

Table 5 Error rate of elastic live load deflection of truss bridge

		5t	10t	15t	18t	21t
D1	y_{C-E}(mm)	59.42	118.84	178.26	213.92	249.57
	y_{N-E}(mm)	51.39	102.78	154.17	185.00	215.84
	y_{M-E}(mm)	48.71	99.52	150.7	186.31	219.56
	δ_{C-E}（mm）	10.71	19.32	27.56	27.61	30.01
	δ_{N-E}（mm）	2.68	3.26	3.47	-1.31	-3.72
	σ_{C-E}	21.99%	19.41%	18.29%	14.82%	13.67%
	σ_{N-E}	5.50%	3.27%	2.30%	-0.70%	-1.69%
D2	y_{C-E}(mm)	81.42	162.83	244.25	293.1	341.94
	y_{N-E}(mm)	67.26	134.51	201.77	242.12	282.48
	y_{M-E}(mm)	63.99	130.23	194.61	242.34	284.12
	δ_{C-E}（mm）	15.19	27.16	38.51	39.47	43.62
	δ_{N-E}（mm）	1.03	-1.16	-3.97	-11.51	-15.84
	σ_{C-E}	22.94%	20.02%	18.72%	15.56%	14.62%
	σ_{N-E}	1.55%	-0.85%	-1.93%	-4.54%	-5.31%
D3	y_{C-E}(mm)	109.14	218.27	327.41	392.89	458.37
	y_{N-E}(mm)	87.31	174.61	261.92	314.31	366.69
	y_{M-E}(mm)	88.79	174.16	263.71	325.38	383.75
	δ_{C-E}（mm）	18.11	38.67	54.57	56.22	60.42
	δ_{N-E}（mm）	-3.72	-4.99	-10.92	-22.36	-31.26
	σ_{C-E}	19.89%	21.53%	20.00%	16.70%	15.18%
	σ_{N-E}	-4.09%	-2.78%	-4.00%	-6.64%	-7.86%
D4	y_{C-E}(mm)	78.15	156.3	234.45	281.34	328.23
	y_{N-E}(mm)	66.72	133.43	200.15	240.17	280.20
	y_{M-E}(mm)	64.62	126.31	190.38	235.87	277.96
	δ_{C-E}（mm）	11.29	24.55	34.94	34.18	36.07
	δ_{N-E}（mm）	-0.14	1.68	0.63	-6.99	-11.96
	σ_{C-E}	16.89%	18.63%	17.51%	13.83%	12.35%
	σ_{N-E}	-0.21%	1.28%	0.32%	-2.83%	-4.09%
D5	y_{C-E}(mm)	58.44	116.88	175.32	210.38	245.44
	y_{N-E}(mm)	50.96	101.91	152.87	183.44	214.01
	y_{M-E}(mm)	45.33	89.45	136.18	169.04	199.93
	δ_{C-E}（mm）	10.87	21.99	30.01	30.05	31.31
	δ_{N-E}（mm）	3.39	7.02	7.56	3.11	-0.12
	σ_{C-E}	22.85%	23.17%	20.65%	16.66%	14.62%
	σ_{N-E}	7.12%	7.40%	5.20%	1.72%	-0.06%

Note:

y_{C-E} is used to calculate live load elastic deflection (without considering the influence of end sleeve on stiffness).

y_{N-E} is used to calculate the live load elastic deflection (considering the influence of the end steel sleeve on stiffness).

y_{M-E} represents the measured live load elastic deflection.

δ_{C-E} represents the error ($\delta_{C-E}=y_{C-E}-y_{M-E}$) obtained without considering the effect of end steel sleeve on stiffness.

δ_{N-E} represents the error ($\delta_{N-E}=y_{N-E}-y_{M-E}$) obtained by considering the effect of end steel sleeve on stiffness.

σ_{C-E} represents the error rate ($\sigma_{C-E}=\delta_{C-E}/y_{M-E}$) obtained without considering the effect of end steel sleeve on stiffness.

σ_{N-E} represents the error rate ($\sigma_{N-E}=\delta_{N-E}/y_{M-E}$) obtained by considering the effect of end steel sleeve on stiffness.

5 Conclusion

In this paper, the load test and deflection calculation method of metal-FRP hybrid space truss bridge are studied. The conclusions are as follows: For metal-FRP hybrid space truss bridge, the material properties of joints have a great influence on the deflection of live load, so the conventional single material truss bridge method can not be used for this new structure. In the calculation of the overall structure, the influence of the steel sleeve at the end of the bar on the stiffness of the bar must be considered. The stiffness equivalent method is used to equivalent the steel sleeve at the end of the bar, which effectively improves the accuracy of the deformation calculation under live load. At the same time, compared with the method of creating solid joint model of the steel sleeve at the end of the bar, the elastic deflection method adopted in this paper is much simpler.

References

1. THOMAS KELLER, YU BAI, TILL VALLEE. Long-Term Performance of a Glass Fiber-Reinforced Polymer Truss Bridge [J]. Joural of Compoites for Construction, 2007, (1): 99 -108.

2. Shao Jinsong, Liu Weiqing, Jiang Tong. Application and Development of Composite Truss in Civil Industry[J]. FRP/CM, 2006, 5:35-39, 54.
3. IWAO SASAKI, ITARU NISHIZAKI. Load-bearing properties of an FRP bridge after nine years of exposure [C]//. CICE 2010-The 5th International Conference on FRP Composites in Civil Engineering, September 27-29, 2010, Beijing, China.
4. V KOSTOPOULOS, YP MARKOPOULOS, DE VLACHOS, et al. A Heavy Duty Composite Bridge Made of Glass/Polyester Pultruded Box Beams[C] //. RTO AVT specialists's meeting on "Low Cost Composite Sructures", May 7-12, 2001, Loen, Norway.
5. V KOSTOPOULOS, YP MARKOPOULOS, DE VLACHOS, et al. Design and Construction of a Vehicular Bridge Made of Glass/Polyester Pultruded Box Beams[J]. Plastics Rubber and Composites, 2005, 34(4): 201-207.
6. Baniya S M. Modeling and Analysis of a Steel Truss Railroad Bridge Traversed by Trains at Various Speeds[J]. Plos Pathogens, 2015, 5(10):10319-10319.
7. Shibeshi R D, Roth C P. Field measurement and dynamic analysis of a steel truss railway bridge[J]. Journal of the South African Institution of Civil Engineers, 2016, 58(3):28-36.
8. Dongdong Zhang,Qilin Zhao,Structural Performance of a Hybrid FRP-Aluminum Modular Triangular Truss System Subjected to Various Loading Conditions,The Scientific World Journal,2014,08.28,2014:1-13.
9. Zhao Qilin, Li Fei, Xu Kang.The static loading experimental study on the new composite truss[J].Industrial Construction, 2011 (S1): 84-87.
10. Qilin Zhao., et al. Research on mechanical properties of a glass fiber reinforced polymer-steel combined truss structure[J]. The Eighth National Academic Conference on FRP application of construction projects. 2013:5.
11. Zhang, D., et al.Flexural properties of a lightweight hybrid FRP-aluminum modular space truss bridge system[J].Composite Structures.2014,108,600 - 615.
12. Jie Tao, Feng Li, Qilin Zhao. Influence of off-axis ply orientationon the axial compressionbehaviour of CFRP tubes[J]. Journal of Reinforced Plastics & Composites, 2016, 0(0) 1–15.
13. Fei Li. Research on new type of pultruded composite connection and application in the truss [D]. Nanjing: PLA University of Science and Technology, 2012.
14. Dasheng Miao. Joint Technology and Structural Properties of FRP Composite Space Truss Bridge[D]. Nanjing: PLA University of Science and Technology, 2013.
15. LI Hui-zhi,YANG Jian-zhong,CHENG Zhan-qi,GUO Yan-bo .Unit-Load Method of Elastic-Plastic Process Analysis of Statically Indeterminate Continuous Beam[J].Chinese Quarterly of Mechanics,2015,(04),721-727